Chapter 42
Effect of Spike-Timing-Dependent Plasticity on Stochastic Spike Synchronization in an Excitatory Neuronal Population

Sang-Yoon Kim and Woochang Lim

Abstract We consider an excitatory population composed of subthreshold neurons which exhibit noise-induced spikings. This neuronal population has adaptive dynamic synaptic strengths governed by the spike-timing-dependent plasticity (STDP). In the absence of STDP, stochastic spike synchronization (SSS) between noise-induced spikings of subthreshold neurons was previously found to occur over a large range of intermediate noise intensities. Here, we investigate the effect of STDP on the SSS by varying the noise intensity. A "Matthew" effect in synaptic plasticity is found to occur due to a positive feedback process. Good synchronization gets better via long-term potentiation (LTP) of synaptic strengths, while bad synchronization gets worse via long-term depression (LTD). Emergence of LTP and LTD of synaptic strengths is investigated through microscopic studies based on both the distributions of time delays between the pre- and the postsynaptic spike times and the pair correlations between the pre- and the postsynaptic IISRs (instantaneous individual spike rates).

Keywords LTD · LTP · Spike-timing-dependent plasticity · Stochastic spike synchronization · Synaptic strength

42.1 Introduction

Recently, much attention has been paid to brain rhythms which emerge via population synchronization between individual firings in neural circuits [1]. These synchronized rhythms are associated with sensory and cognitive processes in the brain. Population synchronization has been intensively investigated in neural

S.-Y. Kim · W. Lim (✉)
Institute for Computational Neuroscience and Department of Science Education, Daegu National University of Education, Daegu, Korea
e-mail: sykim@icn.re.kr; wclim@icn.re.kr

J. M. Delgado-García et al. (eds.), *Advances in Cognitive Neurodynamics (VI)*,
Advances in Cognitive Neurodynamics,
https://doi.org/10.1007/978-981-10-8854-4_42

circuits composed of spontaneously firing suprathreshold neurons exhibiting regular discharges like clock oscillators [2]. In contrast to the case of suprathreshold neurons, the case of subthreshold neurons (which cannot fire spontaneously) has received little attention. The subthreshold neurons can fire only with the help of noise. Here we are interested in stochastic spike synchronization (SSS) (i.e., noise-induced population synchronization) between complex noise-induced firings of subthreshold neurons which exhibit irregular discharges like Geiger counters. Recently, such SSS has been found to occur in an intermediate range of noise intensity via competition between the constructive and the destructive roles of noise [3–6]. In the previous works on SSS, synaptic coupling strengths are static. However, in real brains synaptic strengths may vary (i.e., they can be potentiated or depressed) to adapt to the environment. These adjustments of synapses are called the synaptic plasticity which provides the basis for learning, memory, and development [7]. Regarding the synaptic plasticity, we consider a Hebbian spike-timing-dependent plasticity (STDP) [8–10]. For the STDP, the synaptic strengths vary via a Hebbian plasticity rule depending on the relative time difference between the pre- and the postsynaptic spike times. When a presynaptic spike precedes a postsynaptic spike, long-term potentiation (LTP) occurs; otherwise, long-term depression (LTD) appears. In this paper, we consider an excitatory population of subthreshold neurons and investigate the effect of STDP on the SSS by varying the noise intensity.

42.2 Excitatory Small-World Network of Subthreshold RS Izhikevich Neurons with Synaptic Plasticity

We consider the Watts-Strogatz small-world network (SWN) which interpolates between a regular lattice with high clustering (corresponding to the case of $p = 0$) and a random graph with short average path length (corresponding to the case of $p = 1$) via random uniform rewiring with the probability p [11]. Here, we consider the case that the rewiring probability p is 0.15 and the average number of synaptic inputs per neuron M_{syn} is 20. As an element in our neural system, we choose the regular spiking (RS) Izhikevich neuron model with the same parameters as those in Refs. [12, 13]. Each ith RS Izhikevich neuron is stimulated by using the DC current $I_{DC,i}$ and an independent Gaussian white noise ξ_i whose intensity is controlled by using the parameter D. We also consider a subthreshold case (where only noise-induced firings occur) such that the value of $I_{DC,i}$ is chosen via uniform random sampling in the range of [3.55, 3.65]. The synaptic current into the ith neuron is modeled in terms of the delayed double-exponential functions [14], and the coupling strength of the synapse from the jth presynaptic neuron to the ith postsynaptic neuron is J_{ij}. For the excitatory synapse (involving the AMPA receptors), we use the same synaptic delay, synaptic rise time, synaptic decay time, and synaptic reversal potential as those in [15]. Here, we consider a Hebbian STDP

for the synaptic strengths $\{J_{ij}\}$. Initial synaptic strengths are normally distributed with the mean $J_0(= 0.2)$ and the standard deviation $\sigma = 0.02$. With increasing time the synaptic strength for each synapse is updated with an additive nearest spike pair-based STDP rule:

$$J_{ij} \to J_{ij} + \delta \, \Delta J_{ij}(\Delta t_{ij}), \tag{42.1}$$

where δ $(= 0.005)$ is the update rate and ΔJ_{ij} is the synaptic modification depending on the relative time difference Δt_{ij} $(= t_i^{(\text{post})} - t_j^{(\text{pre})})$ between the nearest spike onsets of the postsynaptic neuron i and the presynaptic neuron j. We use an asymmetric time window for the synaptic modification $\Delta J_{ij}(\Delta t_{ij})$ [9]:

$$\Delta J_{ij} = \begin{cases} A_+ \, e^{-\Delta t_{ij}/\tau_+} \text{ for } \Delta t_{ij} > 0 \\ A_- \, e^{\Delta t_{ij}/\tau_-} \text{ for } \Delta t_{ij} < 0 \end{cases}, \tag{42.2}$$

where $A_+ = 1.0$, $A_- = 0.7$, $\tau_+ = 35\,\text{ms}$, $\tau_- = 70\,\text{ms}$, and $\Delta J_{ij}(\Delta t_{ij} = 0) = 0$. Numerical integration of the governing equations of motion is done using the Heun method [16] (with the time step $\Delta t = 0.01\,\text{ms}$).

42.3 Effect of the STDP on the Stochastic Spike Synchronization

We consider an excitatory Watts-Strogatz SWN of subthreshold RS Izhikevich neurons (exhibiting noise-induced spikings). In the absence of STDP, SSS is found to occur in an intermediate range of noise intensity D. As D passes a lower critical value D_l^* $(\simeq 0.225)$, SSS occurs via the constructive role of noise, while it disappears through the destructive role of noise when passing a higher critical value D_r^* $(\simeq 0.846)$. We take into consideration the STDP, and study its effect on the SSS by varying D, the results of which are well shown in Fig. 42.1. Figure 42.1a shows the time evolution of $\langle J_{ij} \rangle$ for various values of D (chosen in the range of SSS in the absence of STDP), where $\langle J_{ij} \rangle$ represents the population-averaged synaptic strength over all synapses. Initial average strengths at $t = 0$ are $J_0 (= 0.2)$, independently of D. However, with increasing t, $\langle J_{ij} \rangle$ varies (i.e., potentiated or depressed) depending on D. After a sufficiently long time ($\sim$2000 s), $\langle J_{ij} \rangle$ seems to approach its saturated limit value $\langle J_{ij}^* \rangle$. We note that LTP occurs for $D = 0.27$, 0.3, 0.5, and 0.7, while LTD appears for $D = 0.25$ and 0.77. A plot of population-averaged limit values of synaptic strengths $\langle \langle J_{ij}^* \rangle \rangle_r$ vs. D is given in Fig. 42.1b; $\langle \cdots \rangle_r$ represents an average over 20 realizations. Here, the horizontal dotted line denotes the initial values of synaptic strengths J_0 $(= 0.2)$, and the lower and the upper threshold values $\widetilde{D}_l$ $(\simeq 0.253)$ and $\widetilde{D}_r$ $(\simeq 0.717)$ for LTP/LTD are denoted by solid circles. Hence, LTP occurs in the range of $(\widetilde{D}_l, \widetilde{D}_r)$; otherwise, LTD appears. Population spike synchronization may be well visualized in the raster plot of spikes.

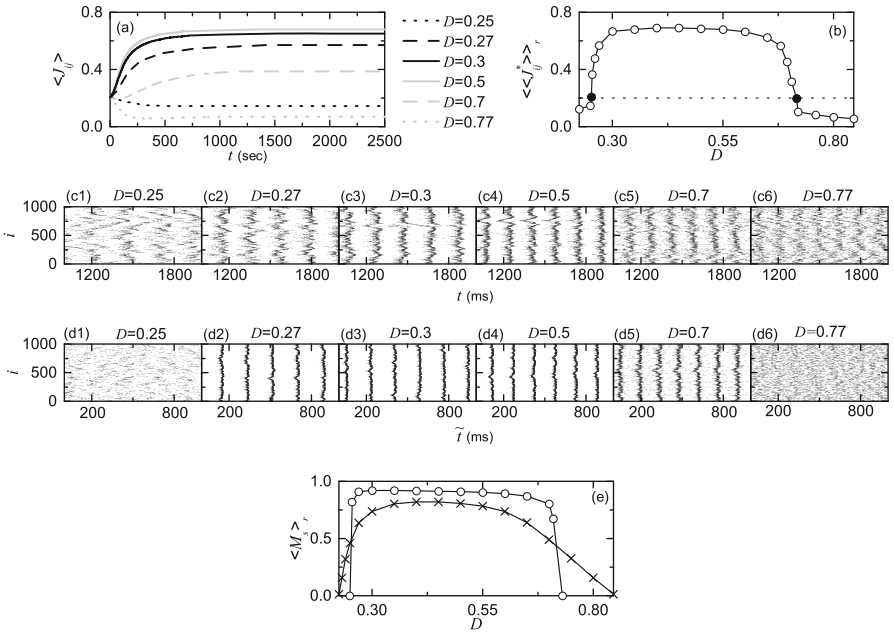

Fig. 42.1 Effect of the STDP on the SSS. (**a**) Time evolution of population-averaged synaptic weight $\langle J_{ij} \rangle$ for various values of D. (**b**) Plot of population-averaged limit value of synaptic weights vs. D. Raster plots of spikes in the absence of STDP [(**c1**)–(**c6**)] and in the presence of STDP [(**d1**)–(**d6**)] [$t = t^*$ (saturation time = 2000 s) $+\tilde{t}$]. (**e**) Plot of the statistical-mechanical spiking measure $\langle M_s \rangle_r$ (represented by open circles) versus D; for comparison, $\langle M_s \rangle_r$ in the absence of the STDP is also shown in crosses

Figure 42.1c1–c6 [Fig. 42.1d1–d6] show the raster plots of spikes in the absence (presence) of STDP. In the case of LTP for $D = 0.27$, 0.3, 0.5 and 0.7, the degree of synchronization is increased. In contrast, for the case of LTD of $D = 0.25$ and 0.77, the population states become unsynchronized. Furthermore, the degree of population synchronization may be quantitatively measured in terms of the realistic statistical-mechanical spiking measure, introduced by considering the occupation pattern and the pacing pattern of the spikes in the spiking stripes in the raster plots of spikes [17]. Figure 42.1e shows plots of $\langle M_s \rangle_r$ in the presence (open circles) and the absence (crosses) of STDP. A "Matthew effect" in the synaptic plasticity seems to occur in the following way. Good synchronization gets better via LTP of synaptic strengths, while bad synchronization gets worse via LTD. As a result, a steplike rapid transition to SSS occurs by varying the noise intensity, in contrast to the relatively smooth transition in the absence of STDP.

We also make an intensive investigation on emergence of LTP and LTD of synaptic strengths via microscopic studies based on both the distributions of time delays $\{\Delta t_{ij}\}$ between the pre- and the postsynaptic spike times and the pair-correlations between the pre- and the postsynaptic instantaneous individual spike

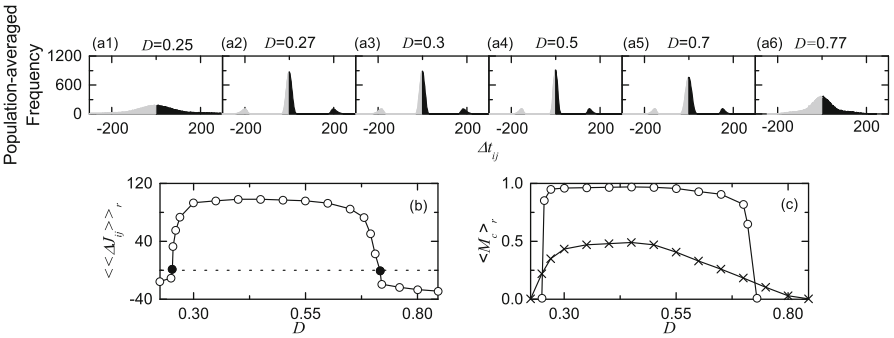

Fig. 42.2 Microscopic investigation on emergence of LTP and LTD via STDP. (**a1**)–(**a6**) Population-averaged histograms for the distributions of time delay Δt_{ij} during the time interval from $t = 0$ to the saturation time ($t = 2000$ s) for various values of D. (**b**) Plot of the population-averaged synaptic modification $\langle\langle \Delta J_{ij} \rangle\rangle_r$ vs. D. (**c**) Plot of the microscopic correlation measure $\langle M_c \rangle_r$ (represented by open circles) versus D in the limiting saturated case; for comparison, $\langle M_c \rangle_r$ in the absence of the STDP is also shown in crosses

rates (IISR) (which is given in Eq. (11) of Ref. [14]). These results are given in Fig. 42.2. Figure 42.2a1–a6 show population-averaged histograms $H(\Delta t_{ij})$ for the distributions of time delay Δt_{ij} during the time interval from $t = 0$ to the saturation time ($t = 2000$ s) for various values of D: for each synaptic pair, its histogram for the distribution of Δt_{ij} is obtained, and then we get the population-averaged histogram via averaging over all synaptic pairs. Here, black and gray regions represent LTP and LTD, respectively. In the case of LTP ($D = 0.27$, 0.3, 0.5, and 0.7), 3 peaks appear: one main central peaks and two minor left and right peaks. When the pre- and the postsynaptic spike times appear in the same spiking stripe in the raster plot of spikes, its time delay Δt_{ij} lies in the main peak; LTP/LTD may occur depending on the sign of Δt_{ij}. On the other hand, time delays Δt_{ij} lie in the minor peaks when the pre- and the postsynaptic spike times appear in the different nearest-neighboring spiking stripes. If the presynaptic stripe precedes the postsynaptic stripe (causality), then its time delay Δt_{ij} lies in the right minor peak (LTP); otherwise, it lies in the left minor peak (LTD). However, in the case of LTD of $D = 0.25$, and 0.77, the population states become desynchronized due to overlap of spiking stripes in the raster plot of spikes. Consequently, the main peak in the histogram becomes merged with the left and the right minor peaks, and then only one broadened main peak appears, in contrast to the case of LTP. The population-averaged synaptic modification $\langle\langle \Delta J_{ij} \rangle\rangle_r$ may be directly obtained from the above histogram $H(\Delta t_{ij})$:

$$\langle\langle \Delta J_{ij} \rangle\rangle_r \simeq \sum_{bins} H(\Delta t_{ij}) \cdot \Delta J_{ij}(\Delta t_{ij}). \tag{42.3}$$

Figure 42.2b shows a plot of $\langle\langle \Delta J_{ij} \rangle\rangle_r$ [obtained from $H(\Delta t_{ij})$] vs. D. Then, population-averaged limit values of synaptic strengths $\langle\langle J_{ij}^* \rangle\rangle_r$ are given by $J_0 + \delta \langle\langle \Delta J_{ij} \rangle\rangle_r$, which agree well with the directly obtained values in Fig. 42.1b. Finally, we study the effect of STDP on the microscopic pair correlation $C_{ij}(\tau)$ between the pre- and the postsynaptic IISRs for the $\langle ij \rangle$ synaptic pair. Then, the microscopic correlation measure M_c, representing the average "in-phase" degree between the pre- and the postsynaptic pairs, is given by the average value of $C_{ij}(0)$ at the zero-time lag for all synaptic pairs. Figure 42.2c shows plots of $\langle M_c \rangle_r$ in the presence (open circles) and the absence (crosses) of STDP. Like the case of M_s, a "Matthew" effect in M_c also occurs: good pair correlation gets better via LTP, while bad pair correlation gets worse via LTD. Hence, a steplike transition occurs, in contrast to the case without STDP. Enhancement in M_c results in the increase in the average in-phase degree between the pre- and the postsynaptic pairs. Then, widths of spiking stripes in the raster plot of spikes decrease, which leads to narrowed distribution of time delays Δt_{ij}. Consequently, LTP may occur. In contrast, for the case of suppression of M_c, the distribution of Δt_{ij} becomes widened, which may lead to occurrence of LTD.

Acknowledgements This research was supported by the Basic Science Research Program through the National Research Foundation of Korea (NRF) funded by the Ministry of Education (Grant No. 20162007688).

References

1. Buzsáki, G.: Rhythms of the Brain. Oxford University Press, New York (2006)
2. Wang, X.-J.: Neurophysiological and computational principles of cortical rhythms in cognition. Physiol. Rev. **90**, 1195–1268 (2010)
3. Wang, Y., Chik, D.T.W., Wang, Z.D.: Coherence resonance and noise-induced synchronization in globally coupled Hodgkin-Huxley neurons. Phys. Rev. E **61**, 740–746 (2000)
4. Lim, W., Kim, S.-Y.: Characterization of stochastic spiking coherence in coupled neurons. J. Korean Phys. Soc. **51**, 1427–1431 (2007)
5. Lim, W., Kim, S.-Y.: Statistical-mechanical measure of stochastic spiking coherence in a population of inhibitory subthreshold neuron. J. Comput. Neurosci. **31**, 667–677 (2011)
6. Kim, S.-Y., Lim, W.: Coupling-induced population synchronization in an excitatory population of subthreshold Izhikevich neurons. Cogn. Neurodyn. **7**, 495–503 (2013)
7. Abbott, L.F., Nelson, S.B.: Synaptic plasticity: taming the beast. Nat. Neurosci. **3**, 1178–1183 (2000)
8. Bi, G.-Q., Poo, M.-M.: Synaptic modifications in cultured hippocampal neurons: dependence on spike timing, synaptic strength, and postsynaptic cell type. J. Neurosci. **18**, 10464–10472 (1998)
9. Song, S., Miller, K.D., Abbott, L.F.: Competitive Hebbian learning through spike-timing-dependent plasticity synaptic plasticity. Nat. Neurosci. **3**, 919–926 (2000)
10. Bi, G.-Q., Poo, M.-M.: Synaptic modification by correlated activity: Hebbs postulate revisited. Annu. Rev. Neurosci. **24**, 139–166 (2001)
11. Watts, D.J., Strogatz, S.H.: Collective dynamics of 'Small-World' networks. Nature **393**, 440–442 (1998)

12. Izhikevich, E.M.: Simple model of spiking neurons. IEEE Trans. Neural Netw. **14**, 1569–1572 (2003)
13. Izhikevich, E.M.: Which model to use for cortical spiking neurons? IEEE Trans. Neural Netw. **15**, 1063–1070 (2004)
14. Kim, S.-Y., Lim, W.: Effect of small-world connectivity on fast sparsely synchronized cortical rhythms. Phys. A **421**, 109–123 (2015)
15. Brunel, N., Wang, X.-J.: What determines the frequency of fast network oscillations with irregular neural discharges? I. Synaptic dynamics and excitation-inhibition balance. J. Neurophysiol. **90**, 415–430 (2003)
16. San Miguel, M., Toral, R.: Stochastic effects in physical systems. In: Martinez, J., Tiemann, R., Tirapegui, E. (eds.) Instabilities and Nonequilibrium Structures VI, pp. 35–130. Kluwer Academic, Dordrecht (2000)
17. Kim, S.-Y., Lim, W.: Realistic thermodynamic and statistical-mechanical measures for neural synchronization. J. Neurosci. Methods **226**, 161–170 (2014)